

Ye Zheng-Hua (Orcid ID: 0000-0001-5714-744X)

Identification of xylan arabinosyl 2-*O*-xylosyltransferases catalyzing the addition of 2-*O*-xylosyl residue onto arabinosyl side chains of xylan in grass species

Ruiqin Zhong¹, Chanhui Lee², Dongtao Cui³, Dennis R. Phillips⁴, Earle R. Adams⁴, Ho-Young Jeong², Ki-Hong Jung⁵ and Zheng-Hua Ye^{1,*}

¹Department of Plant Biology, University of Georgia, Athens, GA 30602, USA

²Department of Plant & Environmental New Resources, College of Life Sciences, Kyung Hee University, Yongin 17104, Republic of Korea

³Department of Chemistry and Chemical Biology, Harvard University, Cambridge, MA 02138, USA

⁴Department of Chemistry, University of Georgia, Athens, GA 30602, USA

⁵Graduate School of Green-Bio Science, Kyung Hee University, Yongin 17104, Republic of Korea

* Corresponding author: E-mail, yh@uga.edu; Fax, 1-706-542-1805
Orcid ID: <https://orcid.org/0000-0001-5714-744X>

Running title: Xylan arabinosyl xylosyltransferase

This is the author manuscript accepted for publication and has undergone full peer review but has not been through the copyediting, typesetting, pagination and proofreading process, which may lead to differences between this version and the Version of Record. Please cite this article as doi: [10.1111/tpj.15939](https://doi.org/10.1111/tpj.15939)

This article is protected by copyright. All rights reserved.

SUMMARY

Grass xylan, being the major hemicellulose in both primary and secondary cell walls, is heavily decorated with α -1,3-linked arabinofuranosyl (Araf) residues that may be further substituted at *O*-2 with xylosyl (Xyl) or Araf residues. Although xylan 3-*O*-arabinosyltransferases (XATs) catalyzing 3-*O*-Araf addition onto xylan have been characterized, glycosyltransferases responsible for the transfer of 2-*O*-Xyl or 2-*O*-Araf onto 3-*O*-Araf residues of xylan to produce the Xyl-Araf and Araf-Araf disaccharide side chains remain to be identified. In this report, we demonstrated that a rice GT61 member, named OsXAXT1 (xylan arabinosyl 2-*O*-xylosyltransferase 1) herein, was able to mediate the addition of Xyl-Araf disaccharide side chains onto xylan when heterologously co-expressed with OsXAT2 in the *Arabidopsis gux1/2/3* (*glucuronic acid substitution of xylan1/2/3*) triple mutant that lacks any glycosyl substitutions. Recombinant OsXAXT1 protein expressed in HEK (human embryonic kidney) 293 cells exhibited a xylosyltransferase activity catalyzing the addition of Xyl from UDP-Xyl onto arabinosylated xylooligomers. Consistent with its function as a xylan arabinosyl 2-*O*-xylosyltransferase, CRISPR-Cas9-mediated mutations of the *OsXAXT1* gene in transgenic rice plants resulted in a reduction in the level of Xyl-Araf disaccharide side chains in xylan. Furthermore, we revealed that XAXT1 close homologs from several other grass species, including switchgrass, maize and *Brachypodium*, possessed the same functions as OsXAXT1, indicating functional conservation of XAXTs in grass species. Together, our findings establish that grass XAXTs are xylosyltransferases catalyzing Xyl transfer onto *O*-2 of Araf residues of xylan to form the Xyl-Araf disaccharide side chains, which furthers our understanding of genes involved in xylan biosynthesis.

Keywords: cell wall, grass, GT61, XAT, XAXT, xylan, xylosyltransferase

Significance Statement

Grass xylan can be substituted at *O*-3 with 2-*O*-Xyl-Araf disaccharide side chains in which the Araf residue may be further esterified with hydroxycinnamates. We have demonstrated that a rice GT61 glycosyltransferase is a xylosyltransferase catalyzing xylosyl transfer onto Araf side chains of xylan, which contributes to our understanding of the biochemical mechanisms underlying the complex substitutions of grass xylan.

INTRODUCTION

Plant lignocellulosic biomass has been exploited as a promising source for production of second-generation biofuels. Among the candidate plant species proposed for biofuel production, grasses represent prominent ones (Marriott et al., 2016). Agriculture residues from extensively cultivated cereal crops, including rice, maize and wheat, as well as dedicated energy grass species, such as switchgrass and miscanthus, are considered to be an abundant renewable source of biomass for biofuel production. However, lignocellulosic biomass is intrinsically recalcitrant to enzymatic degradation, thus hampering its efficient utilization for biofuel production. In particular, grass cell walls contain hydroxycinnamates that crosslink xylan and lignin, which is believed to be one of the key factors contributing to grass biomass recalcitrance (Buanafina 2009; Hatfield et al., 2017). A comprehensive understanding of how grass cell walls are constructed is crucial for custom-designing grass biomass composition suited for biofuel production.

Xylan in grass species constitutes the major hemicellulose in both primary and secondary cell walls and its backbone of β -1,4-linked xylosyl (Xyl) residues is heavily decorated with 3-*O*-arabinofuranosyl (Araf) residues (Vogel, 2008). Other substituents, including 2-*O*-Araf, 2,3-di-*O*-Araf, 2-*O*-glucuronic acid/methylglucuronic acid and 2-*O*/3-*O*-acetyl groups, have also been

found in xylan from various grass species (Hoffmann et al., 1991; Verbruggen et al., 1998; Naran et al., 2009; Mazumder and York, 2010; McCleary et al., 2015; Carvalho et al., 2017; Zhong et al., 2018a). The 3-*O*-Araf residues of grass xylan can be further substituted with a Xyl or an Araf to form the Xyl-Araf or Araf-Araf disaccharide side chains (Kusakabe et al., 1983; Saulnier et al., 1995; Wende and Fry, 1997; Verbruggen et al., 1998; Höjje et al., 2006; Chiniquy et al., 2012; Bowman et al., 2014; Tryfona et al., 2019). In addition, they are often esterified at *O*-5 with hydroxycinnamates, including ferulic acid and *p*-coumaric acid. The ferulate substituents have been shown to mediate cross-links between xylan chains by dimerization and cross-links between xylan and lignin via cross-coupling with coniferyl or sinapyl units of lignin (Hartley et al., 1990; Ralph et al., 1995; Allerdings et al., 2006; de Oliveira et al., 2015; Schendel et al., 2015; Hatfield et al., 2017; Lapierre et al., 2019). The biochemical mechanisms underlying the formation of Xyl-Araf and Araf-Araf disaccharide side chains and hydroxycinnamate esterification of 3-*O*-Araf residues in grass xylan remain elusive.

Genetic and biochemical studies have identified a group of family GT61 glycosyltransferases as xylan 3-*O*-arabinylosyltransferases (XATs) involved in 3-*O*-arabinylosylation of grass xylan. Gain-of-function analyses demonstrated that TaXAT2 from wheat and OsXAT2 to OsXAT7 from rice could mediate the addition of 3-*O*-Araf side chains onto xylan when heterologously expressed in the *Arabidopsis glucuronic acid substitution of xylan1/2/3 (gux1/2/3)* triple mutant (Anders et al., 2012; Zhong et al., 2021). RNAi downregulation of *TaXAT1* in wheat and simultaneous mutations of *OsXAT2* and *OsXAT3* in rice led to reduced arabinylosylation of xylan (Anders et al., 2012; Chen et al., 2021). Activity assays of recombinant proteins of XATs from rice as well as several other grass species, including maize, sorghum, *Brachypodium* and switchgrass, have revealed that they possess

arabinoxyltransferase activities catalyzing Ara^f transfer from UDP-Ara^f onto xylooligomer acceptors (Zhong et al., 2018b and 2021).

Although enzymes responsible for hydroxycinnamate esterification of 3-*O*-Ara^f residues in grass xylan have not been biochemically determined, genetic studies have implicated a group of grass-specific BAHD acyltransferases in this process. Overexpression or RNAi downregulation of several BAHD acyltransferases in *Brachypodium*, *Setaria*, rice and sugarcane resulted in an alteration in the degree of hydroxycinnamate esterification of xylan, leading to the conclusion that they are involved in the transfer of hydroxycinnamates onto xylan (Piston et al., 2010; Bartley et al. 2013; Buanafina et al. 2016; de Souza et al. 2018; Fanelli et al. 2021; Mota et al. 2021). Since these BAHD acyltransferases are cytosol-localized but xylan biosynthesis takes place in the Golgi, it was suggested that they most likely transfer hydroxycinnamates onto UDP-Ara^f to generate the UDP-Ara^f-hydroxycinnamate intermediate, which is then transported into the Golgi where it is used as a donor for the transfer of hydroxycinnamate-esterified Ara^f onto xylan (de Oliveira et al., 2015; Hatfield et al., 2017). However, there is so far no evidence indicating the existence of the proposed UDP-Ara^f-hydroxycinnamate intermediate in plant cells and biochemical proof of the activities of these BAHD acyltransferases is still lacking.

An early study demonstrated that the *xylosyl arabinosyl substitution of xylan 1 (xax1)* mutant was defective in the level of Xyl-Ara^f side chains and the degree of hydroxycinnamate esterification of xylan (Chiniquy et al., 2012), indicating an important role of XAX1, a GT61 glycosyltransferase, in hydroxycinnamate esterification of xylan. Based on the observed mutant chemotypes, it was proposed that XAX1 might be a xylosyltransferase adding Xyl onto the Ara^f residues of xylan to form the Xyl-Ara^f side chains and hydroxycinnamate esterification of Ara^f might occur after Xyl is added onto the Ara^f residues (Chiniquy et al., 2012). However, a recent report showed that rather than a specific reduction of hydroxycinnamate esterification of Ara^f

residues in the Xyl-Araf side chains, the *xax1* mutation caused a general reduction of hydroxycinnamate-esterified Araf in both Araf monosaccharide and Xyl-Araf disaccharide substituents (Feijao et al., 2022). This finding was explained by the suggestion that XAX1 may function as a glycosyltransferase adding hydroxycinnamate-esterified Araf directly onto the xylan backbone and another unknown xylosyltransferase subsequently transfers a Xyl residue onto the hydroxycinnamate-esterified Araf side chains of xylan (Feijao et al., 2022). This proposition seems to be congruent with the proposed functions of the cytosolic BAHD acyltransferases in generating UDP-Araf-hydroxycinnamate that is presumably transported into the Golgi and used as a donor by XAX1. Nevertheless, the actual biochemical function of XAX1 remains unknown and enzymes responsible for the transfer of Xyl onto the Araf residues of xylan to generate the Xyl-Araf disaccharide side chains have not been identified.

In this report, we have demonstrated that a rice GT61 glycosyltransferase, OsXAXT1, is able to transfer Xyl onto *O*-2 of Araf residues of xylan to produce the Xyl-Araf disaccharide side chains when co-expressed with OsXAT2 in the Arabidopsis *gux1/2/3* mutant and its recombinant protein can catalyze the addition of Xyl onto arabinosylated xylooligomers. These results indicate that OsXAXT1 is a xylan arabinosyl 2-*O*-xylosyltransferase, which was further substantiated by CRISPR-Cas9-mediated mutations of the *OsXAXT1* gene showing a reduction of Xyl-Araf disaccharide side chains in xylan. Furthermore, OsXAXT1 close homologs from several other grass species, including switchgrass, *Brachypodium* and maize, were also capable of generating the Xyl-Araf disaccharide side chains in xylan when co-expressed with OsXAT2 in the *gux1/2/3* mutant. Our findings provide additional insights into understanding the complex biochemical process involved in grass xylan substitutions.

RESULTS

Identification of a rice GT61 glycosyltransferase involved in disaccharide substitutions of xylan

Previous studies of rice GT61 members have demonstrated that eight of them, including OsXAT2 to OsXAT7, OsXYXT1 and OsXAX1, mediate 3-*O*-Araf, 2-*O*-Xyl and hydroxycinnamate-esterified 3-*O*-Araf substitutions of xylan, respectively (Anders et al., 2012; Chiniqy et al., 2012; Zhong et al., 2018 and 2021; Feijao et al., 2022). Whether any of the remaining rice GT61 members are involved in xylan substitutions remains elusive. Clade A rice GT61 members phylogenetically fall into five noticeable subgroups (Figure 1a) and at least one member from each of the subgroups I, II III and V has been implicated in xylan substitutions. None of the rice subgroup IV members was able to substitute xylan when heterologously expressed in the Arabidopsis *gux1/2/3* mutant (Zhong et al., 2021). To find out whether any rice subgroup IV GT61 members are involved in the addition of disaccharide side chains (Xyl-Araf or Araf-Araf) onto xylan, we co-expressed them with the xylan 3-*O*-arabinosyltransferase, OsXAT2, in the Arabidopsis *gux1/2/3* mutant, which is ideal for gain-of-function studies of glycosyltransferases involved in xylan substitutions owing to its xylan being devoid of any sugar side chains (Mortimer et al., 2010; Lee et al., 2012). Since expression of OsXAT2 in *gux1/2/3* results in addition 3-*O*-Araf residues onto xylan (Anders et al., 2012; Zhong et al., 2018), we reasoned that if another GT61 member mediates addition of Xyl or Araf onto the Araf residues, its co-expression with OsXAT2 in *gux1/2/3* would lead to generation of the Xyl-Araf or Araf-Araf disaccharide substituents in xylan.

Transgenic plants co-expressing OsXAT2 and rice subgroup IV GT61 members were extracted for alcohol-insoluble cell walls, which were then digested with the GH11 xylanase to release oligosaccharides from xylan for analysis by matrix-assisted laser desorption ionization-

time-of-flight (MALDI-TOF) mass spectrometry. As expected, the xylanase-released oligosaccharides from the *gux1/2/3* mutant only had two ion species (Na^+ adducts) at m/z 629 and 761 (in the range of m/z 500 and 1500) corresponding to the reducing end tetrasaccharide [β -Xyl-(1,3)- α -Rha-(1,2)- α -GalA-(1,4)-xylitol] and pentasaccharide [β -Xyl-(1,4)- β -Xyl-(1,3)- α -Rha-(1,2)- α -GalA-(1,4)-xylitol] sequences, respectively, due to digestion of the unsubstituted xylan backbone into Xyl monomers and dimers, whereas those from *gux1/2/3* expressing OsXAT2 alone displayed an additional ion species at m/z 701 corresponding to arabinosylated xylo-tetraose [(Araf)Xyl₄] (Figure 1b). By contrast, the xylanase-released oligosaccharides from *gux1/2/3* co-expressing OsXAT2 and a subgroup IV GT61 member (Os06g28124), named OsXAXT1 (xylan arabinosyl 2-*O*-xylosyltransferase1) hereafter, showed a new ion species at m/z 833 in addition to those corresponding to arabinosylated xylo-tetraose and the reducing end tetra- and penta-saccharide sequences (Figure 1b). This new ion species had an increase in mass over the mass of (Araf)Xyl₄ by 132 Da, which corresponds to a Xyl or an Araf residue (after the loss of water), and hence it could be attributed to (Araf)Xyl₄ that is further xylosylated or arabinosylated. Since expression of OsXAXT1 alone in *gux1/2/3* did not result in any new ion species compared with the *gux1/2/3* mutant (Figure 1b), it indicates that OsXAXT1 does not directly xylosylate or arabinosylate the xylan backbone; instead, it is most likely involved in addition of Xyl or Araf onto the Araf side chains of xylan. Among the five rice subgroup IV members, OsXAXT1 is the only one that when co-expressed with OsXAT2 in *gux1/2/3*, led to the appearance of the new ion species at m/z 833 compared with *gux1/2/3* expressing OsXAT2 alone.

Xylan from *gux1/2/3* co-expressing OsXAXT1 and OsXAT2 contains Xyl-Araf disaccharide side chains

We next employed ^1H nuclear magnetic resonance (NMR) spectroscopy to determine whether the xylooligomers from *gux1/2/3* co-expressing OsXAXT1 and OsXAT2 contained the Xyl-Araf or Araf-Araf disaccharide side chains (Figure 1c). As expected, the xylanase-released oligosaccharides from the *gux1/2/3* mutant only had resonances corresponding to the xylan reducing end sequences [β -Xyl-(1,3)- α -Rha-(1,2)- α -GalA-(1,4)-xylitol and β -Xyl-(1,4)- β -Xyl-(1,3)- α -Rha-(1,2)- α -GalA-(1,4)-xylitol] but lacked resonances of reducing terminal Xyl due to its reduction into xylitol by NaBH_4 during xylan extraction with KOH. Xylooligomers from *gux1/2/3* expressing OsXAT2 alone displayed additional resonances corresponding to the backbone Xyl residues and a resonance signal at 5.39 ppm that is characteristic of H1 of terminal Araf (Figure 1c). By contrast, the xylooligomers from *gux1/2/3* co-expressing OsXAXT1 and OsXAT2 exhibited a new resonance signal at 5.539 ppm (Figure 1c), which is a diagnostic signal of H1 of 2-*O*-substituted Araf (Höjje et al., 2006), in addition to the resonances corresponding to terminal Araf and the backbone Xyl residues. Consistent with the MALDI-TOF MS data, the xylanase-released oligosaccharides from *gux1/2/3* expressing OsXAXT1 alone did not show any additional resonances compared with the *gux1/2/3* mutant (Figure 1c). It is noteworthy that the resonances for terminal Araf and 2-*O*-substituted Araf observed in the xylooligomers from *gux1/2/3* co-expressing OsXAXT1 and OsXAT2 were also present in the xylooligomers from wild-type rice xylan (Figure 1c). These ^1H NMR results demonstrated that the xylooligomers from *gux1/2/3* co-expressing OsXAXT1 and OsXAT2 contained Araf side chains that are further substituted at *O*-2. Integration analysis of the resonance signals showed an average ratio of 1:5 between 2-*O*-substituted Araf and total Araf, indicating that about 20% of Araf residues are substituted at *O*-2.

We next aimed to decipher the identity of the substituent at *O*-2 of the Araf side chains. Because the xylanase-released oligosaccharides from *gux1/2/3* co-expressing OsXAXT1 and

OsXAT2 were a mixture of oligosaccharides seen as ion species at m/z 629, 701, 761, and 833 in the MALDI-TOF mass spectra (Figure 1b), we undertook to separate the oligosaccharide at m/z 833, which corresponds to substituted (Araf)Xyl₄, from the other ones. Since the xylan reducing end tetra- and penta-saccharide sequences are acidic, they were removed by anion exchange chromatography, leaving only the neutral xylooligomers corresponding to the MALDI-TOF MS ion species at m/z 701 (sequence 1) and 833 (sequence 2) (Figure 2a). The sequence 1 and sequence 2 xylooligomers were further separated by size exclusion chromatography and verified by MALDI-TOF MS (Figure 2a) before subjected to structure analysis by ¹H NMR spectroscopy. It was found that sequence 1 had a resonance signal characteristic of H1 of terminal α -Araf at 5.39 ppm in addition to those corresponding to the backbone β -Xyl residues (Figure 2b), thus confirming its substitution with an α -Araf residue. By contrast, besides the resonances of the backbone β -Xyl residues, sequence 2 exhibited a predominant resonance signal at 5.539 ppm attributed to H1 of α -Araf substituted at O-2 (Figure 2b). Noticeably, it also displayed resonances at 4.546 ppm (Figure 2b), which are characteristic of H1 of terminal β -Xyl linked to O-2 of Araf (Höjje et al., 2006). The neutral xylooligomer mixture before separation of the two sequences had resonance signals of both sequence 1 and sequence 2 (Figure 2b). The finding that sequence 2 exhibited resonance signals at 5.539 ppm attributed to H1 of α -Araf substituted at O-2 and at 4.546 ppm corresponding to H1 of terminal β -Xyl linked to O-2 of Araf indicates that it is substituted with the Xyl-Araf disaccharide (Figure 2c).

To further corroborate the ¹H NMR data showing the presence of the Xyl-Araf disaccharide substituent in sequence 2, we carried out two-dimensional (2D) NMR experiments, including heteronuclear single quantum coherence (HSQC), heteronuclear two-bond correlation (H2BC) and heteronuclear multiple bond correlation (HMBC), to assign and compare the resonance signals for the Xyl and Araf residues in sequences 1 and 2 (Figure 3). Examination of

the HSQC spectra revealed that although both sequences 1 and 2 had resonances attributed to the one-bond H1-C1 correlations of the backbone β -Xyl1 to β -Xyl4 residues, sequence 1 also displayed the expected resonances attributed to the H1-C1 correlation of terminal α -Araf side chains (H1 at 5.39 ppm and C1 at 107.5 ppm) and sequence 2 exhibited distinct resonances attributed to the H1-C1 correlations of the side-chain β -Xyl5 (H1 at 4.546 ppm and C1 at 102.5 ppm) and 2-*O*-substituted α -Araf (H1 at 5.539 ppm and C1 at 106.3 ppm) residues (Figure 3a,b). Furthermore, the H2BC spectra showed that while the resonances corresponding to the two-bond H1-C2 correlations of the backbone β -Xyl1 to β -Xyl4 residues were apparent in both sequences, those attributed to the H1-C2 correlation of the side-chain β -Xyl5 (H1 at 4.546 ppm and C2 at 72.7 ppm) were only present in sequence 2 (Figure 3a,b).

The glycosidic linkages of the side chains in sequences 1 and 2 were further validated by HMBC, which provides correlations between carbons and protons that are separated by two or more bonds. Both sequences 1 and 2 had resonances corresponding to the correlation between H1 of α -Araf and C3 of β -Xyl3 and that between C1 of α -Araf and H3 of β -Xyl3 (Figure 3c,d), verifying the linkage of α -Araf to *O*-3 of the backbone β -Xyl3 residue. By contrast, sequence 2 displayed additional resonances corresponding to the correlation between H1 of β -Xyl5 at 4.546 ppm and C2 of α -Araf at 88.6 ppm and that between C1 of β -Xyl5 at 102.5 ppm and H2 of α -Araf at 4.256 ppm (Figure 3d), confirming the substitution of α -Araf at *O*-2 with β -Xyl5 in sequence 2 (Figure 2c). Based on the 2D NMR data of sequences 1 and 2, their spectra were assigned (Figure 3e,f). The assignments for the backbone β -Xyl residues, the terminal α -Araf residue and the β -Xyl- α -Araf side chain in sequences 1 and 2 are congruent with those published previously (Höjje et al., 2006). The fact that the C2 resonance of α -Araf in sequence 2 had a large deshielding to 88.6 ppm compared to that of α -Araf in sequence 1 at 80.6 ppm (Figure 3e,f)

is consistent with the conclusion that the α -Araf residue in sequence 2 is substituted at *O*-2 (Höjje et al., 2006). Together, these 2D NMR data have established that the sequence 2 xylooligomer from *gux1/2/3* co-expressing OsXAXT1 and OsXAT2 is xylooligomer substituted at *O*-3 with a β -Xyl-(1 \rightarrow 2)- α -Araf disaccharide chain, indicating that OsXAXT1 mediates the transfer of 2-*O*-Xyl onto the Araf side chains of xylan.

OsXAXT1 is a Golgi-localized xylosyltransferase catalyzing the addition of Xyl onto Araf side chains of xylan

OsXAXT1 is predicted to be a type II membrane protein with an N-terminal transmembrane helix followed by a putative catalytic domain (Figure S1). Green fluorescence protein (GFP)-tagged OsXAXT1 was found to be co-localized with mCherry-tagged Fringe Fiber8 (FRA8), a known Golgi-localized glycosyltransferase, when they were co-expressed in Arabidopsis protoplasts (Figure 4a), indicating that OsXAXT1 resides in the Golgi where xylan biosynthesis occurs. To biochemically determine whether OsXAXT1 is a xylosyltransferase mediating addition of Xyl onto the Araf side chains of xylan, we generated recombinant OsXAXT1 protein in the human embryonic kidney (HEK) 293 cells for its enzymatic activity assay (Figs. 4b and S2). Recombinant OsXAXT1 was incubated with the UDP-Xyl donor and the arabinosylated xylooligomer acceptor (Araf)Xyl₄ and the reaction products were examined by MALDI-TOF mass spectrometry. It was found that in addition to the ion species at *m/z* 701 corresponding to the (Araf)Xyl₄ acceptor, the OsXAXT1-catalyzed reaction products had a new ion species at *m/z* 833 with a mass increase of 132 Da (corresponding to one Xyl residue) over the mass of (Araf)Xyl₄ (Figure 4c), indicating that OsXAXT1 is able to transfer a Xyl residue onto the (Araf)Xyl₄ acceptor. By contrast, incubation of OsXAXT1 with UDP-Araf and the (Araf)Xyl₄ acceptor did not result in addition of Araf onto the acceptor (Figure 4c). Furthermore,

OsXAXT1 could not transfer Xyl or Araf onto anthranilic acid (AA)-labeled xylohexaose (Xyl6-AA) from UDP-Xyl or UDP-Araf (Figure 4d), which is consistent with the gain-of-function analysis showing that OsXAXT1 is unable to directly xylosylate or arabinosylate the xylan backbone. These biochemical analyses suggest that OsXAXT1 is a xylosyltransferase catalyzing the transfer of Xyl onto the Araf side chains of xylan (Figure 4e).

CRISPR/Cas9-mediated mutations of *OsXAXT1* in rice result in a reduction in the level of 2-*O*-substituted Araf residues in xylan

The finding that OsXAXT1 is involved in the addition of Xyl at *O*-2 of Araf side chains of xylan prompted us to investigate whether its mutation could impact the level of 2-*O*-substituted Araf residues in xylan *in vivo*. To generate *OsXAXT1* mutants, we employed the CRISPR-Cas9-mediated gene editing approach using two guide RNAs, gRNA1 and gRNA2, targeting two different sites in the fourth exon of the *OsXAXT1* gene (Figure 5a). Two independent homozygous mutant lines, *xaxt1-1* and *xaxt1-2*, harboring different mutations in the *OsXAXT1* gene (Figure 5b,c), were used for structural analysis of xylan. While the *xaxt1-2* mutation had a 12-bp deletion resulting in a deletion of 4 amino acids (#495 to 498) in the putative catalytic domain, the *xaxt1-1* mutation caused a 1-bp deletion leading to a frameshift after tyrosine 265 and thus a truncation of 269 amino acids in the putative catalytic domain and an addition of 47 aberrant amino acids before a premature stop codon is encountered (Fig. S3). No changes in plant growth and development were observed in the mutants compared with the wild type (Figure S4). ¹H NMR analysis of xylanase-released xylooligomers from wild-type rice and the *xaxt1* mutants revealed the presence of resonance signals characteristic of terminal Araf residues at 5.39 ppm and 2-*O*-substituted Araf residues at 5.539 ppm in addition to resonances corresponding to the backbone Xyl residues (Figure 5d). Integration of the resonance signals

demonstrated that although no alterations were seen in the ratio of total *Araf* residues to total Xyl residues in the *xaxt1* mutants compared with the wild type, the percentage of 2-*O*-substituted *Araf* over total *Araf* residues in the *xaxt1* mutants was reduced to about 78.7% of that of the wild type (Figure 5d), indicating that mutations of the *OsXAXT1* gene led to a reduction in the level of 2-*O*-substituted *Araf* side chains in xylan. This finding is consistent with the results from the gain-of-function studies and biochemical analysis of *OsXAXT1* showing its involvement in Xyl transfer onto the *Araf* side chains of xylan. The moderate reduction of 2-*O*-substituted *Araf* side chains of xylan in the *xaxt1* mutants suggests functional redundancy of *OsXAXT1* with other uncharacterized glycosyltransferases in xylosylating the *Araf* side chains of xylan.

XAXT1 homologs from switchgrass, *Brachypodium* and maize are able to add Xyl-*Araf* side chains onto xylan when co-expressed with *OsXAT2* in the *gux1/2/3* mutant

A BLAST search revealed that *OsXAXT1* homologs exist in the genomes of other grass species, including switchgrass, *Brachypodium*, maize and sorghum, and they are phylogenetically clustered into two subgroups (Figure 6a). To determine whether they possess the same function as *OsXAXT1*, we first attempted to express their recombinant proteins in HEK293 cells for activity assay but were unsuccessful. Therefore, we resorted to the gain-of-function approach to investigate whether these grass XAXT homologs were able to xylosylate *Araf* side chains of xylan when co-expressed with *OsXAT2* in the *gux1/2/3* mutant. ¹H NMR analyses of xylanase-released xylooligomers from transgenic *gux1/2/3* plants revealed that compared with *gux1/2/3* expressing *OsXAT2* alone, co-expression of *OsXAT2* with subgroup I XAXT homologs from switchgrass (*PvXAXT1* and *PvXAXT2*), *Brachypodium* (*BdXAXT1*) or maize (*ZmXAXT1*) resulted in the appearance of new resonances at 5.539 ppm that is characteristic of 2-*O*-substituted *Araf* and resonances at 4.546 ppm corresponding to Xyl

attached to *O*-2 of *Araf* side chains (Figure 6b). These new resonances were not observed in xylanase-released oligosaccharides from *gux1/2/3* co-expressing OsXAT2 and subgroup II XAXT homologs from switchgrass (Pavir.4KG250000, Pavir.4NG167700, Pavir.1NG52200 and Pavir.1NG519600) or sorghum (Sobic.004G320600) (Figure S5). These results indicate that the xylooligomers from *gux1/2/3* co-expressing OsXAT2 and PvXAXT1, PvXAXT2, BdXAXT1 or ZmXAXT1 have 2-*O*-Xyl-substituted *Araf* side chains.

We next employed 2D-HSQC NMR analysis to verify the presence of 2-*O*-Xyl-substituted *Araf* side chains in the xylooligomers from *gux1/2/3* co-expressing OsXAT2 and PvXAXT1, PvXAXT2, BdXAXT1 or ZmXAXT1. It was evident that these xylooligomers had distinct resonances corresponding to the H1-C1 correlation of 2-*O*-substituted *Araf* (H1 at 5.539 ppm and C1 at 106.3 ppm) and the H1-C1 correlation of Xyl attached to *O*-2 of *Araf* side chains (H1 at 4.546 ppm and C1 at 102.5 ppm) compared to the xylooligomers from *gux1/2/3* expressing OsXAT2 only (Figure 7). As expected, the resonances corresponding to the H1-C1 correlations of terminal *Araf* and the four backbone Xyl residues were present in all samples (Figure 7). These results suggest that like OsXAXT1, these grass XAXTs are also xylosyltransferases catalyzing Xyl transfer onto *O*-2 of *Araf* side chains of xylan.

DISCUSSION

Grass xylan is heavily substituted with 3-*O*-*Araf* side chains, some of which can be further decorated at *O*-2 with Xyl or *Araf*. Although an early study suggested that rice XAX1 was likely responsible for Xyl transfer onto the *Araf* residues of xylan to generate the Xyl-*Araf* side chains (Chiniquy et al., 2012), a recent report proposes that XAX1 functions to transfer hydroxycinnamate-esterified *Araf* residues onto xylan based on the finding that the *xax1* mutant has a general reduction of hydroxycinnamate-esterified *Araf* residues in xylan regardless of

whether *Araf* is substituted with Xyl or not (Feijao et al., 2022). Therefore, glycosyltransferases involved in the transfer of Xyl or *Araf* onto the 3-*O-Araf* residues of xylan to form the Xyl-*Araf* and *Araf-Araf* disaccharide side chains remain elusive. In this report, using both genetic and biochemical approaches, we have investigated the function of a rice GT61 member, OsXAXT1, and demonstrated that it is a xylosyltransferase mediating Xyl transfer onto the *Araf* residues of xylan to form the Xyl-*Araf* disaccharide side chains.

We have revealed through a combination of MALDI-TOF MS, 1D and 2D NMR analyses that although xylan from the *gux1/2/3* mutant expressing OsXAT2 alone only has 3-*O-Araf* side chains, xylan from *gux1/2/3* co-expressing OsXAXT1 and OsXAT2 contains 2-*O-Xyl*-substituted *Araf* side chains, indicating that OsXAXT1 mediates Xyl transfer onto the *Araf* side chains of xylan. In addition, recombinant OsXAXT1 protein expressed in HEK293 cells was able to catalyze the transfer of Xyl from UDP-Xyl onto the arabinosylated xylo-tetraose acceptor. A role of OsXAXT1 in substitutions of the *Araf* residues of xylan was further substantiated by CRISPR/Cas9-mediated mutations of *OsXAXT1* in transgenic rice showing a reduction in the level of 2-*O*-substituted *Araf* residues in xylan. These multiple lines of data establish that OsXAXT1 is a xylan arabinosyl 2-*O*-xylosyltransferase catalyzing the transfer of 2-*O-Xyl* residues onto the *Araf* side chains of xylan.

It was noted that the rice *xaxt1* mutants only had a moderate reduction in the level of 2-*O*-substituted *Araf* residues in xylan, suggesting a redundancy of genes responsible for xylosylation of the *Araf* side chains of xylan. Such a gene redundancy has previously been reported for other rice glycosyltransferase genes involved in xylan biosynthesis. For example, there are six IRX10 homologs in rice and mutation of one of them, OsIRX10, resulted in approximately 10% reduction in Xyl content in the cell walls compared with the wild type (Chen et al., 2013). Similarly, six OsXATs have been identified in rice (Zhong et al., 2021) and

simultaneous mutations of two of them, OsXAT2 and OsXAT3, caused about 30% reduction in Araf content in rice cell walls compared with the wild type (Chen et al., 2021). It is currently unknown which other rice GT61 members may play a redundant role with OsXAXT1 in xylosylating the Araf side chains of xylan. Although Os02g22190 is phylogenetically closely related to OsXAXT1 (Figure 1a), its co-expression with OsXAT2 in the *gux1/2/3* mutant did not result in 2-*O*-substitutions of the Araf residues of xylan and its recombinant protein expressed in HEK293 cells was unable to xylosylate the arabinosylated xylotetraose acceptor (Figure S6), implying that its biochemical function might differ from that of OsXAXT1. It is possible that similar to the scenario of OsXATs, which belong to different subgroups (Zhong et al., 2021; Figure 1a), some GT61 members residing in other subgroups may share redundant functions with OsXAXT1. It remains to be investigated which GT61 members might possess the same enzymatic activity as OsXAXT1.

The Xyl-Araf disaccharide side chain has been identified in xylan from a number of grass species, implying that it is a common substitution in grass xylan (Kusakabe et al., 1983; Saulnier et al., 1995; Wende and Fry, 1997; Höjje et al., 2006; Chiniqy et al., 2012; Bowman et al., 2014; Tryfona et al., 2019). We have demonstrated that the close homologs of OsXAXT1 from switchgrass, maize and *Brachypodium* are able to produce the Xyl-Araf disaccharide side chains in xylan when co-expressed with OsXAT2 in the *gux1/2/3* mutant. This finding indicates that they are functional orthologs of OsXAXT1 involved in xylosylating the Araf side chains of xylan, which is consistent with the presence of Xyl-Araf disaccharide chains in xylan of these species. It is interesting to note that grass XAXT1 homologs fall into two subgroups; while subgroup I members are functional orthologs of OsXAXT1, subgroup II members were unable to xylosylate the Araf side chains of xylan when co-expressed with OsXAT2 in the *gux1/2/3* mutant (Figure S5). The fact that the only sorghum homolog is not a functional ortholog of OsXAXT1

suggests that if sorghum xylan has Xyl-Araf side chains, other GT61 members most likely mediate Xyl transfer onto the Araf residues.

Members of the GT61 family previously characterized biochemically are all involved in addition of Araf or Xyl side chains directly on the xylan backbone (Anders et al., 2012; Zhong et al., 2018 and 2021). Our study of XAXTs reveals that further substitutions of the Araf side chains by Xyl is also catalyzed by GT61 members. It is envisioned that additional grass GT61 members may also mediate glycosyl substitutions of grass xylan, such as 2-*O*-Araf, 2,3-di-*O*-Araf and Araf-Araf. Further functional studies of grass GT61 glycosyltransferases will promise to advance our understanding of the complex substitutions of grass xylan.

EXPERIMENTAL PROCEDURES

Phylogenetic analysis

Amino acid sequences of rice GT61 members were retrieved from the rice genome database in Phytozome v13. The genomes of switchgrass, *Brachypodium*, maize, and sorghum in Phytozome v13 were BLAST-searched for close homologs of OsXAXT1. The phylogenetic relationships of GT61 members were evaluated using The MEGA (v6.0) software with the maximum likelihood method.

Generation of transgenic *Arabidopsis gux1/2/3* plants co-expressing OsXAT2 and other GT61 members

The full-length cDNAs of *OsXAT2* and other GT61 genes driven by the 2-kb *CesA7* promoter were ligated into a modified pGPTV binary vector to generate the expression constructs. The primers used for PCR amplification of the full-length cDNAs were 5'-atgaagcccgtc g a g c g c c c a a g-3' and 5'-ctattgattcaattgatcaagaac-3' for *OsXAT2*, 5'-

cggatggttagcca gtccaagac g-3' and 5'-ctatcccctgagcatttgaa gac-3' for *OsXAXT1*, 5'-aggatggtc gcc gactcttcttgg-3' and 5'-ctatccccggatcgtcc ggagcac-3' for *BdXAXT1*, 5'-cggatggttagcca gtccaagac g-3' and 5'-ctatcccctgagcatttgaa gac-3' for *ZmXAXT1*, 5'-gggatgggcacc gactc gcc gtc g-3' and 5'-ctattccttgagcatctggagcac-3' for *PvXAXT1*, 5'-gggatgggc gccacc gactggcc g-3' and 5'-ttattccctgagcatctggagcac-3' for *PvXAXT2*. For co-expression of a GT61 member with *OsXAT2*, the expression cassette of the GT61 gene was inserted into a cloning site in the *OsXAT2* expression construct to create the co-expression construct. The constructs were introduced into the *Arabidopsis gux1/2/3* mutant plants by *Agrobacterium*-mediated transformation. At least 60 independent transgenic plants were generated for each expression construct. No apparent alterations in plant growth were observed in transgenic *gux1/2/3* plants expressing these GT61 members compared with the *gux1/2/3* mutant. Stems from three separate pools of 20 independent transgenic plants, each of them representing a biological replicate, were collected for xylan structure analyses.

Cell wall preparation and xylanase digestion

Alcohol-insoluble cell walls were isolated from the transgenic *Arabidopsis* and rice plants as previously described (Lee et al., 2007). The isolated cell walls were extracted with KOH for xylan, which was then digested with xylanase to release xylooligomers according to Zhong et al. (2005). Briefly, 0.1 g of alcohol-insoluble cell walls from *Arabidopsis* or rice were incubated with 1 N KOH in the presence of 1% sodium borohydride. After neutralization and lyophilization, the KOH extracts were digested with endo-1,4- β -xylanase M6 from rumen microorganism (Megazyme). The xylanase digests were passed through a Sephadex G25 column (1x100 cm; GE Healthcare, IL, USA) and the xylooligomers were collected for subsequent structural analyses by MALDI-TOF MS and NMR spectroscopy. For removal of the acidic

reducing end sequences, xylanase-released xylooligomers were passed through a DEAE-Sepharose column (0.5x15cm; GE Healthcare). The resulting neutral xylooligomers were further passed through a Bio-Gel P-2 column (1x100 cm; Bio-Rad, CA, USA) to separate sequence 1 and sequence 2 according to Mazumder and York (2010).

MALDI-TOF MS

Xylooligomers and the reaction products were examined for their masses by MALDI-TOF MS using a Burkert Autoflex TOF mass spectrometer (Billerica, MA, USA) in reflection mode (Lee et al., 2007). The spectra were the averages of at least 200 laser shots. Samples from three biological replicates were analyzed and representative spectra were shown.

NMR spectroscopy

The xylooligomers were analyzed with Varian Inova 500 MHz and Agilent DD2 600 MHz NMR spectrometers. One-dimensional and two-dimensional (HSQC, H2BC and HMBC) NMR spectra were recorded using standard Varian pulse sequences. The proton positions and residue identities in the NMR spectra were assigned based on our 1D and 2D NMR spectral data and the published NMR spectral data for xylan (Höjje et al., 2006; Chiniquy et al. 2012).

Xylooligomers isolated from three separate pools of samples were examined.

Expression of recombinant OsXAXT1 protein in HEK293 cells

The putative catalytic domain of OsXAXT1 (amino acids 61 to 534) was expressed as a secreted His-tagged recombinant protein in HEK293 cells (Zhong et al. 2017). The corresponding sequence of the *OsXAXT1* cDNA was PCR-amplified with the gene-specific primers (5'-tctcggaggatgccattgtgagg-3' and 5'-ctatcccctgagcatttgaagcac-3'), cloned in frame

between the murine Igk chain leader sequence and the c-myc epitope and six tandem histidine tags in the pSecTag2 mammalian expression vector (Invitrogen) and confirmed by sequencing. The expression construct was transfected into HEK293 cells using the Invitrogen FreeStyle 293 Expression System. After culturing the transfected cells for 5 days, the culture medium was collected and passed through a nickel resin column for purification of His-tagged recombinant protein. The purified recombinant OsXAXT1 was examined by SDS-PAGE and Coomassie Blue staining.

Activity assays of recombinant OsXAXT1

The purified recombinant OsXAXT1 (20 μ g) was incubated with 0.3 mM arabinosylated xylo-tetraose [(Araf)Xyl₄] or anthranilic acid (AA)-labeled xylohexaose as acceptors, 1 mM UDP-Xyl (CarboSource) or UDP-Araf (Peptide Institute) as donors, and 1 mM MgCl₂ in 50 mM HEPES buffer (pH 7.0) at 37 °C for 16 hr. The arabinosylated xylo-tetraose acceptor was purified from xylanase-digested cell walls of transgenic *gux1/2/3* plants expressing OsXAT2. Xylohexaose was labeled at its reducing terminus with AA according to Ishii et al. (2002). The reaction products were analyzed using MALDI-TOF mass spectrometry after passing through Dowex 1X4 resin.

Subcellular localization of OsXAXT1

OsXAXT1 was tagged with green fluorescent protein (GFP) at its C-terminus and cloned under the cauliflower mosaic virus (CaMV) 35S promoter in a modified pBI221 vector. OsXAXT1-GFP was co-expressed with a Golgi marker, mCherry-tagged FRA8 (Zhong et al., 2005), in Arabidopsis leaf protoplasts (Yoo et al., 2007) and the fluorescent signals in transfected

Arabidopsis protoplasts were recorded using a Zeiss LSM 710 confocal microscope. At least 10 Arabidopsis protoplasts were imaged and representative images were shown.

CRISPR-Cas9-mediated mutations of *OsXAXT1* in rice plants

The specific target sequences for CRISPR-Cas9-mediated mutations of *OsXAXT1* were selected using the CRISPRdirect software (<https://crispr.dbcls.jp>; Naito et al., 2015). The target sequences (gRNA1 and gRNA2) were ligated into the *BsaI* site of the pRGEB32 binary vector (Addgene plasmid ID 63142). The constructs were introduced into rice (*Oryza sativa* ssp. *japonica* cv. Dongjin) via *Agrobacterium*-mediated transformation (Lee et al., 1999) for generation of transgenic rice plants. Genomic DNA was isolated from leaves of 1-month-old T1 transgenic plants for genotyping by sequencing of PCR-amplified *OsXAXT1* gene to identify transgenic plants with target mutations. Sixteen transgenic rice T1 lines for each of the gRNA1 and gRNA2 targets were genotyped. Among the 16 lines generated with gRNA1, 3 had homozygous mutations, 9 heterozygous mutations and 4 no mutations. Among the 16 lines generated with gRNA2, 4 lines had homozygous mutations, 8 heterozygous mutations and 4 no mutations. Homozygous transgenic T2 mutant plants were selected and the leaves and leaf sheaths of 3-month-old plants were used for cell wall extraction and subsequent xylan structure analysis.

ACCESSION NUMBERS

The Genbank accession numbers/the gene locus names of the genes studied in this report are ON932575/Os06g28124 for *OsXAXT1*, ON932576/Bradi3g09797 for *BdXAXT1*,

ON932577/Zm00001d045972 for ZmXAXT1, ON932578/Pavir.4KG221000 for PvXAXT1, and ON932579/Pavir.4NG080700 for PvXAXT2.

ACKNOWLEDGMENTS

This work was supported by the U.S. Department of Energy, Office of Science, Basic Energy Sciences under award No. DE-FG02-03ER15415. CL was supported by the National Research Foundation of Korea (NRF) grant (NRF-2020R1A2C1004273). We thank Dr. M.K. Kandasamy at the UGA Biomedical Microscopy Core for assistance with imaging using the Zeiss LSM 710 confocal microscope.

AUTHOR CONTRIBUTION

RZ and ZHY conceived and designed research. RZ, CL, DC, DRP, ERA, HYJ, KHJ and ZHY conducted experiments and analyzed data. RZ and ZHY wrote the manuscript. All authors read and approved the manuscript.

CONFLICT OF INTEREST

The authors declare no conflict of interest.

DATA AVAILABILITY

All data generated during this study are included in this article and its Supplementary Figure files.

SUPPORTING INFORMATION

Supplementary Figures S1-S6 are available in the accompanying supplementary file.

Figure S1. OsXAXT1 is predicted to be a type II membrane protein with an N-terminal transmembrane helix.

Figure S2. SDS-PAGE and Coomassie Blue staining of nickel resin-bound proteins from the culture medium of untransfected control HEK293 cells.

Figure S3. Diagrams of the wild-type OsXAXT1 protein and the *xaxt1-1* and *xaxt1-2* mutant proteins.

Figure S4. Morphology of a wild-type rice plant (left) and the two independent homozygous mutants, *xaxt1-1* (middle) and *xaxt1-2* (right), generated by CRISPR-Cas9-mediated editing of the *OsXAXT1* gene.

Figure S5. ¹H NMR spectra of xylooligomers isolated from transgenic *gux1/2/3* plants co-expressing OsXAT2 and subgroup II XAXT homologs from sorghum (Sobic) or switchgrass (Pavir).

Figure S6. The recombinant protein of Os02g22190 was unable to transfer Xyl or Ara_f onto the (Ara_f)Xyl₄ acceptor.

REFERENCES

- Allerdings, E., Ralph, J., Steinhart, H. and Bunzel, M. (2006) Isolation and structural identification of complex feruloylated heteroxylan side-chains from maize bran. *Phytochemistry*, 67, 1276-1286.
- Anders, N., Wilkinson, M.D., Lovegrove, A., Freeman, J., Tryfona, T., Pellny, T.K. et al. (2012) Glycosyl transferases in family 61 mediate arabinofuranosyl transfer onto xylan in grasses. *Proc. Natl. Acad. Sci. USA*, 109, 989-993.

- Bartley, L.E, Peck, M.L., Kim, S.R., Ebert, B., Manisseri, C., Chiniqy, D.M., et al. (2013)** Overexpression of a BAHD acyltransferase, OsAt10, alters rice cell wall hydroxycinnamic acid content and saccharification. *Plant Physiol.*, 161, 1615-1633.
- Bowman, M.J., Dien, B.S., Vermillion, K.E. and Mertens, J.A. (2014)** Structural characterization of (1→2)-β-xylose-(1→3)-α-arabinose-containing oligosaccharide products of extracted switchgrass (*Panicum virgatum*, L.) xylan after exhaustive enzymatic treatment with α-arabinofuranosidase and β-endo-xylanase. *Carbohydr. Res.*, 398, 63-71.
- Buanafina, M.M. (2009)** Feruloylation in grasses: current and future perspectives. *Mol. Plant*, 2, 861-872.
- Buanafina, M.M., Fescemyer, H.W., Sharma, M. and Shearer, E.A. (2016)** Functional testing of a PF02458 homologue of putative rice arabinoxylan feruloyl transferase genes in *Brachypodium distachyon*. *Planta*, 243, 659-674.
- Carvalho, D.M., Martínez-Abad, A., Evtuguin, D.V., Colodette, J.L., Lindström, M.E., Vilaplana, F. et al. (2017)** Isolation and characterization of acetylated glucuronoarabinoxylan from sugarcane bagasse and straw. *Carbohydr. Polym.*, 156, 223-234.
- Chen, C., Zhao, X., Wang, X., Wang, B., Li, H., Feng, J. and Wu, A. (2021)** Mutagenesis of UDP-xylose epimerase and xylan arabinosyl-transferase decreases arabinose content and improves saccharification of rice straw. *Plant Biotechnol. J.*, 19, 863-865.
- Chiniqy, D., Sharma, V., Schultink, A., Baidoo, E.E., Rautengarten, C., Cheng, K. et al. (2012)** XAX1 from glycosyltransferase family 61 mediates xylosyltransfer to rice xylan. *Proc. Natl. Acad. Sci. USA*, 109, 17117-17122.
- Fanelli, A., Rancour, D.M., Sullivan, M., Karlen, S.D., Ralph, J., Riaño-Pachón, D.M. et al. (2021)** Overexpression of a sugarcane BAHD acyltransferase alters hydroxycinnamate content in maize cell wall. *Front. Plant Sci.*, 12, 626168.

- Feijao, C., Morreel, K., Anders, N., Tryfona, T., Busse-Wicher, M., Kotake, T. et al.** (2022) Hydroxycinnamic acid modified xylan side chains and their cross-linking products in rice cell walls are reduced in the *Xylosyl arabinosyl substitution of xylan 1* mutant. *Plant J.*, 109, 1152-1167.
- Hartley, R.D., Morrison, W.H.III, Himmelsbach, D.S. and Borneman, W.S.** (1990) Cross-linking of cell wall phenolic arabinoxylans in graminaceous plants. *Phytochemistry*, 29, 3705-3709.
- Hatfield, R.D., Rancour, D.M. and Marita, J.M.** (2017) Grass cell walls: a story of cross-linking. *Front. Plant Sci.*, 7, 2056.
- Hoffmann, R.A., Leeftang, B.R., de Barse, M.M., Kamerling, J.P. and Vliegthart, J.F.** (1991) Characterisation by ¹H-n.m.r. spectroscopy of oligosaccharides, derived from arabinoxylans of white endosperm of wheat, that contain the elements $\rightarrow 4$)[α -L-Araf-(1->3)]- β -D-Xylp-(1-> or $\rightarrow 4$)[α -L-Araf-(1->2)][α -L-Araf-(1->3)]- β -D-Xylp-(1->. *Carbohydr. Res.*, 221, 63-81.
- Höije, A., Sandstrom, C., Roubroeks, J.P., Andersson, R., Gohil, S. and Gatenholm, P.** (2006) Evidence of the presence of 2-O- β -D-xylopyranosyl- α -L-arabinofuranose side chains in barley husk arabinoxylan. *Carbohydr. Res.*, 341, 2959-2966.
- Ishii, T., Ichita, J., Matsue, H., Ono, H. and Maeda, I.** (2002) Fluorescent labeling of pectic oligosaccharides with 2-aminobenzamide and enzyme assay for pectin. *Carbohydr. Res.*, 337, 1023-1032.
- Kusakabe, I., Ohgushi, S., Yasui, T. and Kobayashi, T.** (1983) Structures of the arabinoxylo-oligosaccharides from the hydrolytic products of corncob arabinoxylan by a xylanase from *Streptomyces*. *Agric. Biol. Chem.*, 47, 2713-2723.

- Lapierre, C., Voxeur, A., Boutet, S. and Ralph, J.** (2019) Arabinose conjugates diagnostic of ferulate-ferulate and ferulate-monolignol cross-coupling are released by mild acidolysis of grass cell walls. *J. Agri. Food Chem.*, 67, 12962-12971.
- Lee, S., Jeon, J.S., Jung, K.H. and An, G.** (1999) Binary vectors for efficient transformation of rice. *J. Plant Biol.*, 42, 310-316.
- Lee, C., Teng, Q., Zhong, R. and Ye, Z.-H.** (2012) Arabidopsis GUX proteins are glucuronyltransferases responsible for the addition of glucuronic acid side chains onto xylan. *Plant Cell Physiol.*, 53, 1204-1216.
- Lee, C., Zhong, R., Richardson, E.A., Himmelsbach, D.S., McPhail, B.T. and Ye, Z.H.** (2007) The PARVUS gene is expressed in cells undergoing secondary wall thickening and is essential for glucuronoxylan biosynthesis. *Plant Cell Physiol.*, 48, 1659-1672.
- Marriott, P.E., Gómez, L.D., McQueen-Mason, S.J.** (2016) Unlocking the potential of lignocellulosic biomass through plant science. *New Phytol.*, 209, 1366-1381.
- Mazumder, K. and York, W.S.** (2010) Structural analysis of arabinoxylans isolated from ball-milled switchgrass biomass. *Carbohydr. Res.*, 345, 2183-2193.
- McCleary, B.V., McKie, V.A., Draga, A., Rooney, E., Mangan, D. and Larkin, J.** (2015) Hydrolysis of wheat flour arabinoxylan, acid-debranched wheat flour arabinoxylan and arabinoxylo-oligosaccharides by β -xylanase, α -L-arabinofuranosidase and β -xylosidase. *Carbohydr. Res.*, 407, 79-96.
- Mortimer, J.C., Miles, G.P., Brown, D.M., Zhang, Z., Segura, M.P., Weimar, T. et al.** (2010) Absence of branches from xylan in Arabidopsis *gux* mutants reveals potential for simplification of lignocellulosic biomass. *Proc. Natl. Acad. Sci. USA*, 107, 17409-17414.

- Mota, T.R., de Souza, W.R., Oliveira, D.M., Martins, P.K., Sampaio, B.L., Vinecky, F. et al.** (2021) Suppression of a BAHD acyltransferase decreases *p*-coumaroyl on arabinoxylan and improves biomass digestibility in the model grass *Setaria viridis*. *Plant J.*, 105, 136-150.
- Naito, Y., Hino, K., Bono, H. and Ui-Tei, K.** (2015) CRISPRdirect: software for designing CRISPR/Cas guide RNA with reduced off-target sites. *Bioinformatics*, 31, 1120-1123.
- Naran, R., Black, S., Decker, S.R. and Azadi, P.** (2009) Extraction and characterization of native heteroxylans from delignified corn stover and aspen. *Cellulose*, 16, 661-675.
- de Oliveira, D.M., Finger-Teixeira, A., Mota, T.R., Salvador, V.H., Moreira-Vilar, F.C., Molinari, H.B.C. et al.** (2015) Ferulic acid: a key component in grass lignocellulose recalcitrance to hydrolysis. *Plant Biotechnol. J.*, 13, 1224-1232.
- Piston, F., Uauy, C., Fu, L., Langston, J., Labavitch, J. and Dubcovsky, J.** (2010) Down-regulation of four putative arabinoxylan feruloyl transferase genes from family PF02458 reduces ester-linked ferulate content in rice cell walls. *Planta*, 231, 677-691.
- Ralph, J., Grabber, J.H. and Hatfield, R.D.** (1995) Lignin-ferulate cross-links in grasses: active incorporation of ferulate polysaccharide esters into ryegrass lignins. *Carbohydr. Res.*, 275, 167-178.
- Schendel, R.R., Meyer, M.R. and Bunzel, M.** (2015) Quantitative profiling of feruloylated arabinoxylan side-chains from graminaceous cell walls. *Front. Plant Sci.*, 6, 1249.
- Saulnier, L., Vigouroux, J. and Thibault, J.-F.** (1995) Isolation and partial characterization of feruloylated oligosaccharides from maize bran. *Carbohydr. Res.*, 272, 241-253.
- de Souza, W.R., Martins, P.K., Freeman, J., Pellny, T.K., Michaelson, L.V., Sampaio, B.L. et al.** (2018) Suppression of a single BAHD gene in *Setaria viridis* causes large, stable decreases in cell wall feruloylation and increases biomass digestibility. *New Phytol.*, 218, 81-93.

- Tryfona, T., Sorieul, M., Feijao, C., Stott, K., Rubtsov, D.V., Anders, N. et al.** (2019) Development of an oligosaccharide library to characterise the structural variation in glucuroarabinoxylan in the cell walls of vegetative tissues in grasses. *Biotechnol. Biofuels*, 12, 109.
- Verbruggen, M.A., Spronk, B.A., Schols, H.A., Beldman, G., Voragen, A.G., Thomas, J.R., et al.** (1998) Structures of enzymically derived oligosaccharides from sorghum glucuroarabinoxylan. *Carbohydr. Res.*, 306, 265-274.
- Vogel, J.** (2008) Unique aspects of the grass cell wall. *Curr. Opin. Plant Biol.*, 11, 301-307.
- Wende, G. and Fry, S.C.** (1997) 2-*O*- β -D-Xylopyranosyl-(5-*O*-feruloyl)-L-arabinose, a widespread component of grass cell walls. *Phytochemistry*, 44, 1019-1030.
- Yoo, S.D., Cho, Y.H. and Sheen, J.** (2007) Arabidopsis mesophyll protoplasts: a versatile cell system for transient gene expression analysis. *Nat. Protoc.*, 2, 1565-1572.
- Zhong, R., Cui, D., Dasher, R.L. and Ye, Z.-H.** (2018a) Biochemical characterization of rice xylan *O*-acetyltransferases. *Planta*, 247, 1489-1498.
- Zhong, R., Cui, D., Phillips, D.R., Sims, N.T. and Ye, Z.-H.** (2021) Functional analysis of GT61 glycosyltransferases from grass species in xylan substitutions. *Planta*, 254, 131.
- Zhong, R., Cui, D., Phillips, D.R. and Ye, Z.-H.** (2018b) A novel rice xylosyltransferase catalyzes the addition of 2-*O*-xylosyl side chains onto the xylan backbone. *Plant Cell Physiol.*, 59, 554-565.
- Zhong, R., Cui, D. and Ye, Z.-H.** (2017) Regiospecific acetylation of xylan is mediated by a group of DUF231-containing *O*-acetyltransferases. *Plant Cell Physiol.*, 58, 2126-2138.
- Zhong, R., Cui, D. and Ye, Z.-H.** (2019) Secondary cell wall biosynthesis. *New Phytol.*, 221, 1703-1723.

Zhong, R., Peña, M.J., Zhou, G.-K., Nairn, C.J., Wood-Jones, A., Richardson, E.A. et al.

(2005) *Arabidopsis Fragile Fiber8*, which encodes a putative glucuronyltransferase, is essential for normal secondary wall synthesis. *Plant Cell*, 17, 3390-3408.

Figure Legends

Figure 1. Gain-of-function analysis of OsXAXT1 for its ability to substitute Araf side chains of xylan by its co-expression with OsXAT2 in the *Arabidopsis gux1/2/3* mutant. (a) Phylogenetic relationship of clades A members of the rice (*Oryza sativa*) GT61 family. The phylogenetic tree was constructed using the maximum likelihood method and the 0.1 scale indicates a 10% change. The numbers at nodes are bootstrap values (percentages) from 1,000 replicates. Os08g39380 from the GT61 clade C was included as an outgroup. The GT61 members are shown with their locus identifiers and names if available. OsXAXT1 characterized in this report is highlighted in yellow. (b) MALDI-TOF mass spectra of xylooligomers isolated from transgenic *gux1/2/3* plants expressing OsXAXT1, OsXAT2 or both. Each ion peak is denoted with its mass ($[M+Na]^+$). The ion species at m/z 629 and 761 correspond to the reducing end tetra- and penta-saccharide sequences, respectively. Note the appearance of a new ion species at m/z 833 (highlighted in pink) in xylooligomers from *gux1/2/3* co-expressing OsXAXT1 and OsXAT2 compared with those from *gux1/2/3* expressing OsXAT2 alone. (c) 1H NMR spectra of xylooligomers from *gux1/2/3* expressing OsXAXT1, OsXAT2 or both. The 1H NMR spectrum of xylooligomers from rice xylan was included for comparison. Resonance peaks are marked with proton positions and the corresponding residue identities. The resonances attributed to the xylan reducing end sequence (α -GalA, α -Rha and 3-linked β -Xyl) are indicated in grey. Note that similar to those of rice xylan, xylooligomers from *gux1/2/3* co-expressing OsXAXT1 and OsXAT2 exhibited resonances corresponding to H1 of 2-*O*-substituted α -Araf at 5.539 ppm (highlighted in pink) in

addition to those corresponding to H1 of 3-*O*-linked terminal α -Araf at 5.39 ppm (highlighted in green) seen in xylooligomers from *gux1/2/3* expressing OsXAT2 only. HDO, hydrogen deuterium oxide.

Figure 2. Structural analysis of xylooligomers from *gux1/2/3* co-expressing OsXAXT1 and OsXAT2. (a) MALDI-TOF mass spectra of neutral xylooligomers isolated from *gux1/2/3* co-expressing OsXAXT1 and OsXAT2 before (left panel) and after separation of the sequence 1 (middle panel) and sequence 2 (right panel) xylooligomers corresponding to the ion species at m/z 701 and 833 ($[M+Na]^+$), respectively. (b) 1H NMR spectra of sequence 1 and sequence 2 in comparison with that of xylooligomers before their separation. Resonance peaks are marked with proton positions and the corresponding residue identities. Note that in addition of the resonances corresponding to H1 of the backbone Xyl1 to Xyl4 residues, sequence 1 (middle spectrum) displayed a resonance signal corresponding to H1 of 3-*O*-linked terminal α -Araf at 5.39 ppm (highlighted in green), whereas sequence 2 (bottom spectrum) exhibited resonances attributed to H1 of 2-*O*-substituted α -Araf at 5.539 ppm (highlighted in pink) and H1 of Xyl5 that is attached to *O*-2 of α -Araf at 4.546 ppm (highlighted in yellow). (c) Diagram of the sequence 2 xylooligomer, which is xylotetraose (Xyl1 to Xyl4) substituted at *O*-3 with an Araf that is further decorated at *O*-2 with a Xyl (Xyl5).

Figure 3. 2D NMR analyses of the glycosidic linkages in the sequence 1 and sequence 2 xylooligomers. Resonance peaks are marked with proton and carbon positions and the corresponding residue identities. (a) and (b) HSQC and H2BC spectra showing one-bond H1-C1 correlations and two-bond H1-C2 correlations, respectively, between 1H and ^{13}C of each Xyl residue and Araf in sequence 1 (a) and sequence 2 (b). Note the appearance of the H1-C1

(HSQC) and H1-C2 (H2BC) signals for Xyl5 in sequence 2 (highlighted in yellow). (c) and (d) HMBC spectra showing interglycosidic cross-peaks between H1 and ^{13}C in sequence 1 (c) and sequence 2 (d). Note the cross-peak resonances between H1 of Araf and C3 of Xyl3 and those between H3 of Xyl3 and C1 of Araf in sequence 1 (highlighted in green), and the cross-peak resonances between H1 of Araf and C3 of Xyl3, those between H3 of Xyl3 and C1 of Araf, those between H1 of Xyl5 and C2 of Araf and those between H2 of Araf and C1 of Xyl5 in sequence 2 (highlighted in yellow). (e) and (f) Assignment of ^1H and ^{13}C NMR chemical shifts of sequence 1 (e) and sequence 2 (f) based on their 1D and 2D NMR spectra. The diagnostic ^1H and ^{13}C NMR chemical shifts for terminal α -Araf (H1/C1), 2-*O*-substituted α -Araf (H1/C1 and H2/C2) and β -Xyl5 (H1/C1) are highlighted in yellow. ND, resonances not determined.

Figure 4. Subcellular localization and enzymatic activity assay of OsXAXT1. (a) Confocal images of GFP and mCherry fluorescent signals in a protoplast co-expressing GFP-tagged OsXAXT1 and mCherry-tagged FRA8. Note the co-localization of the punctate signals of GFP and mCherry (merged). DIC, differential interference contrast. Scale bars = 9 μm . (b) SDS-PAGE and Coomassie Blue staining of recombinant OsXAXT1 protein expressed in HEK293 cells. The molecular masses of markers are shown on the left. The lower band is most likely a proteolytic degradation product of OsXAXT1. (c) and (d) MALDI-TOF mass spectra of OsXAXT1-catalyzed reaction products. OsXAXT1 was incubated with the arabinosylated xylo-tetraose [(Araf)Xyl₄] acceptor (c) or the anthranilic acid (AA)-labeled xylohexaose (Xyl₆-AA) acceptor (d) in the absence of UDP-sugars (control) or in the presence of UDP-Araf or UDP-Xyl. Each ion species is denoted with its mass ($[\text{M}+\text{Na}]^+$) and oligomer composition. Note that only the reaction products from OsXAXT1 incubated with (Araf)Xyl₄ and UDP-Xyl had a new ion species at m/z 833 with an increased mass of 132 Da (corresponding to one Xyl residue)

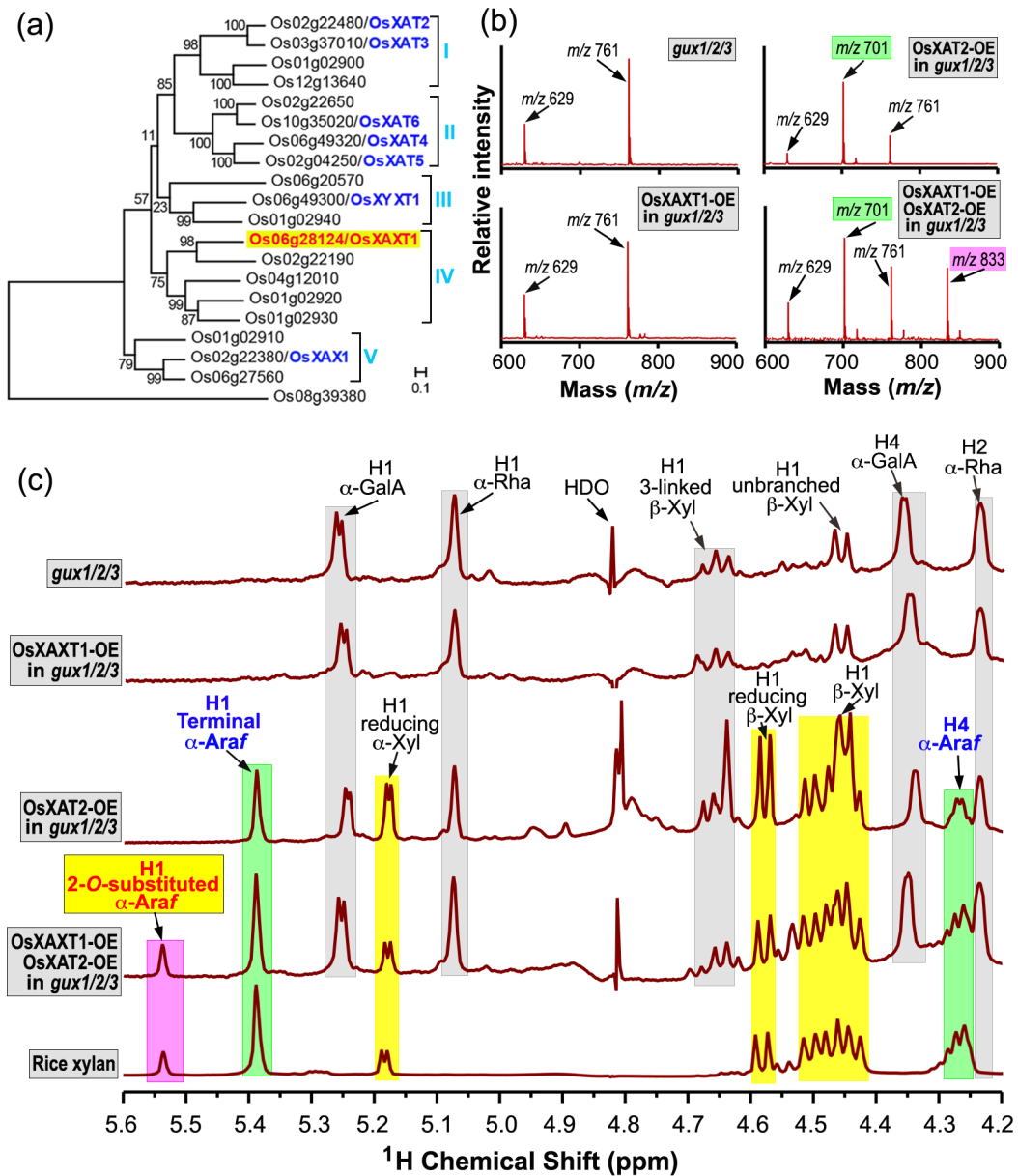
over the mass of the acceptor. (e) Schematic diagram depicting OsXAXT1 catalyzed Xyl transfer onto the Ara_f residue of the (Ara_f)Xyl₄ acceptor.

Figure 5. Effect of CRISPR/Cas9-mediated mutation of *OsXAXT1* on 2-*O*-substitutions of the Ara_f side chains in rice xylan. (a) Diagram of the *OsXAXT1* gene showing the positions targeted by the two guide RNAs (gRNA1 and gRNA2) used for CRISPR/Cas9-mediated editing of the *OsXAXT1* gene. (b) Deletion mutations of the *OsXAXT1* gene in the two homozygous mutant lines, *xaxt1-1* and *xaxt1-2*, at the respective gRNA1 and gRNA2 target sites. The deleted bases are indicated in red and the protospacer-adjacent motif (PAM) is boxed in yellow. (c) DNA sequence chromatograms of the gRNA1 and gRNA2 target sites of *OsXAXT1* showing the deletion mutations in *xaxt1-1* and *xaxt1-2* compared with the wild type (WT). The PAM motif is boxed in purple lines and the deleted nucleotides are boxed in red lines. (d) ¹H NMR spectra of xylooligomers from the *xaxt1-1* and *xaxt1-2* mutant compared with those from WT. Resonance peaks are marked with proton positions and the corresponding residue identities. The percentage of H1 of 2-*O*-substituted Ara_f over H1 of total Ara_f (sum of H1 of 2-*O*-substituted Ara_f and H1 of terminal Ara_f) was calculated by integration of the corresponding resonance peaks and shown at right of the panel. The data are the mean ± se of three biological replicates.

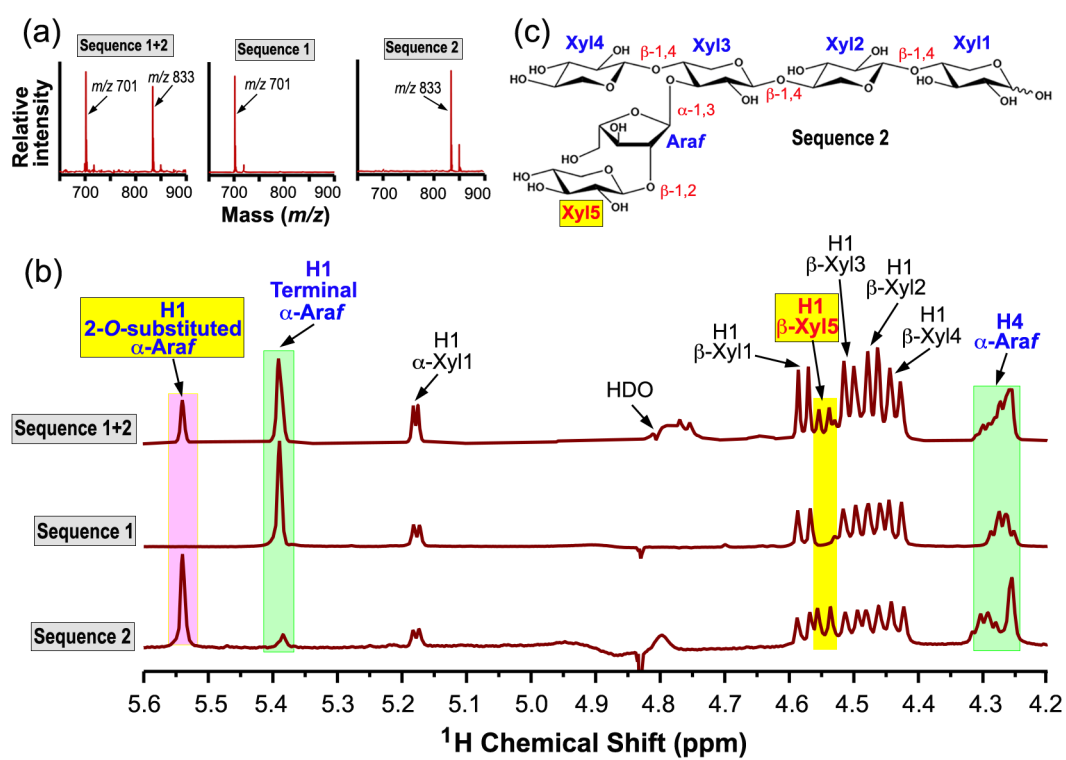
Figure 6. Gain-of-function analysis of grass XAXT homologs by their co-expression with OsXAT2 in the Arabidopsis *gux1/2/3* mutant. (a) Phylogenetic relationship of OsXAXT1 homologs from switchgrass (*Panicum virgatum*; Pv/Pavir), maize (*Zea mays*; Zm), *Brachypodium* (*Brachypodium distachyon*; Bd/Bradi) and sorghum (*Sorghum bicolor*; Sb/Sobic). A rice GT61 member, Os02g22190, which is closely related to OsXAXT1 (Figure 1a) and its close homologs from several other grasses were used as an outgroup. The phylogenetic tree was

constructed using the maximum likelihood method and the 0.1% scale indicates a 10% change. The numbers at nodes are bootstrap values (percentages) from 1,000 replicates. (b) ^1H NMR spectra of xylooligomers from *gux1/2/3* co-expressing OsXAT2 and grass XAXT homologs. Resonance peaks are marked with proton positions and the corresponding residue identities. See Figure 2c for the numbering of Xyl residues. Note that compared with the xylooligomers from *gux1/2/3* expressing OsXAT2 alone, those from *gux1/2/3* co-expressing OsXAT2 and XAXT homologs from switchgrass (PvXAXT1 and PvXAXT2), *Brachypodium* (BdXAXT1) or maize (ZmXAXT1) exhibited additional resonances corresponding to H1 of 2-*O*-substituted α -Araf at 5.539 ppm (highlighted in pink) and H1 of Xyl attached to *O*-2 of α -Araf at 4.546 ppm (highlighted in yellow).

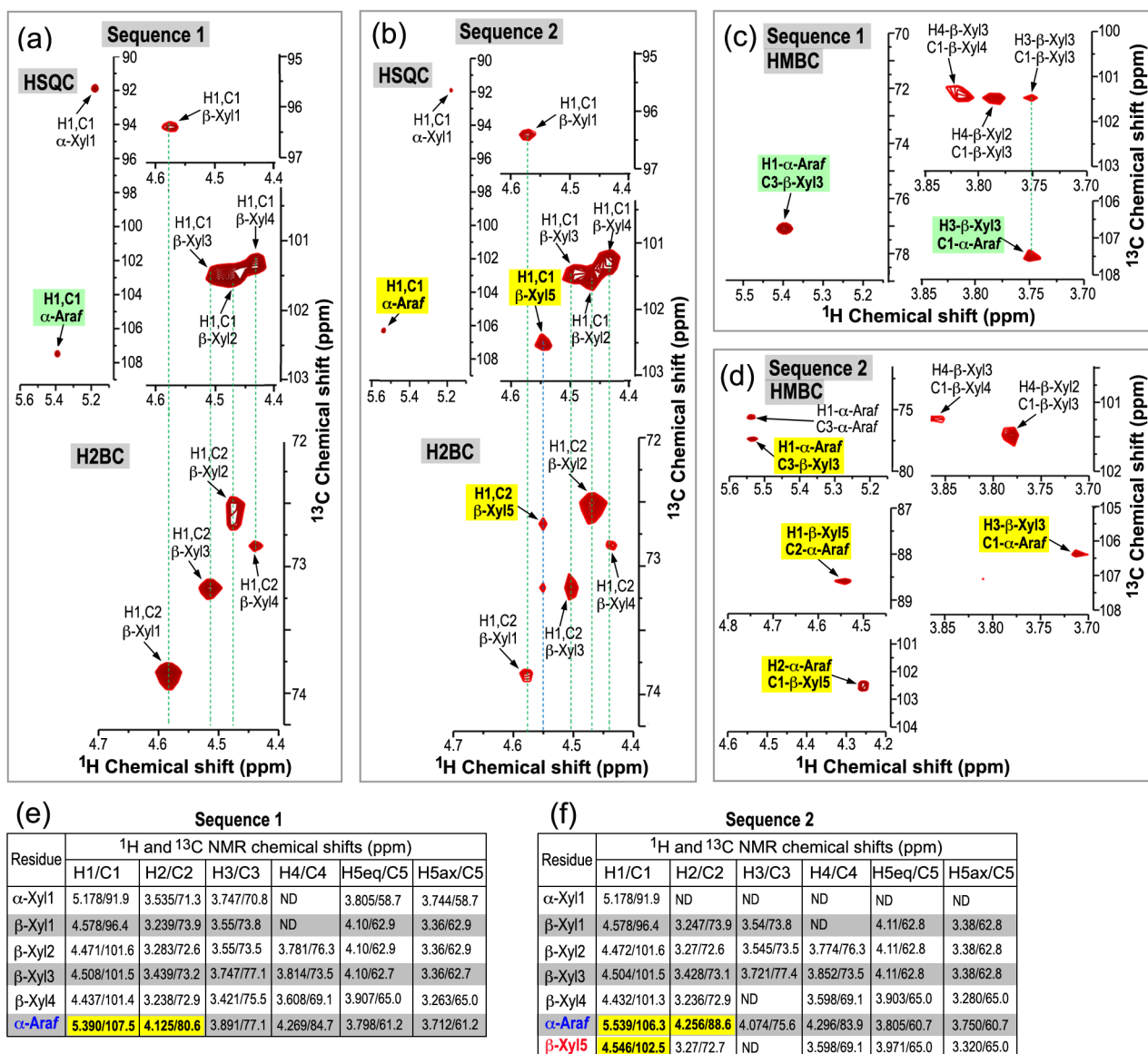
Figure 7. 2D-HSQC NMR analysis of one-bond H1-C1 correlations between ^1H and ^{13}C of each Xyl residue and Araf in xylooligomers from *gux1/2/3* co-expressing OsXAT2 and grass XAXT homologs. Resonance peaks are marked with proton and carbon positions and the corresponding residue identities. See Figure 2C for the numbering of Xyl residues. (a) HSQC spectra of xylooligomers from *gux1/2/3* expressing OsXAT2 only. Note the H1-C1 signals for Xyl1 to Xyl4 and terminal α -Araf. (b) to (e) HSQC spectra of xylooligomers from *gux1/2/3* co-expressing OsXAT2 and XAXT homologs from switchgrass [PvXAXT1(b) and PvXAXT2 (c)], *Brachypodium* [BdXAXT1 (d)] or maize [ZmXAXT1 (e)]. Note the appearance of the new H1-C1 signals for 2-*O*-substituted α -Araf (highlighted in green) and those for Xyl5 attached to *O*-2 of α -Araf (highlighted in yellow) in (b) to (e).



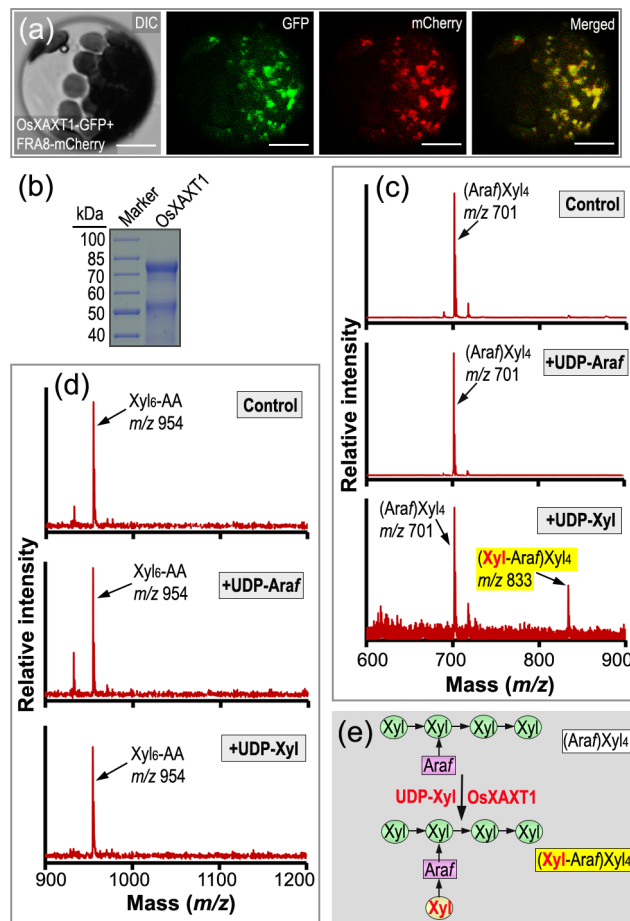
TPJ_15939_Fig.1-C1-G1-NMR copy.tif



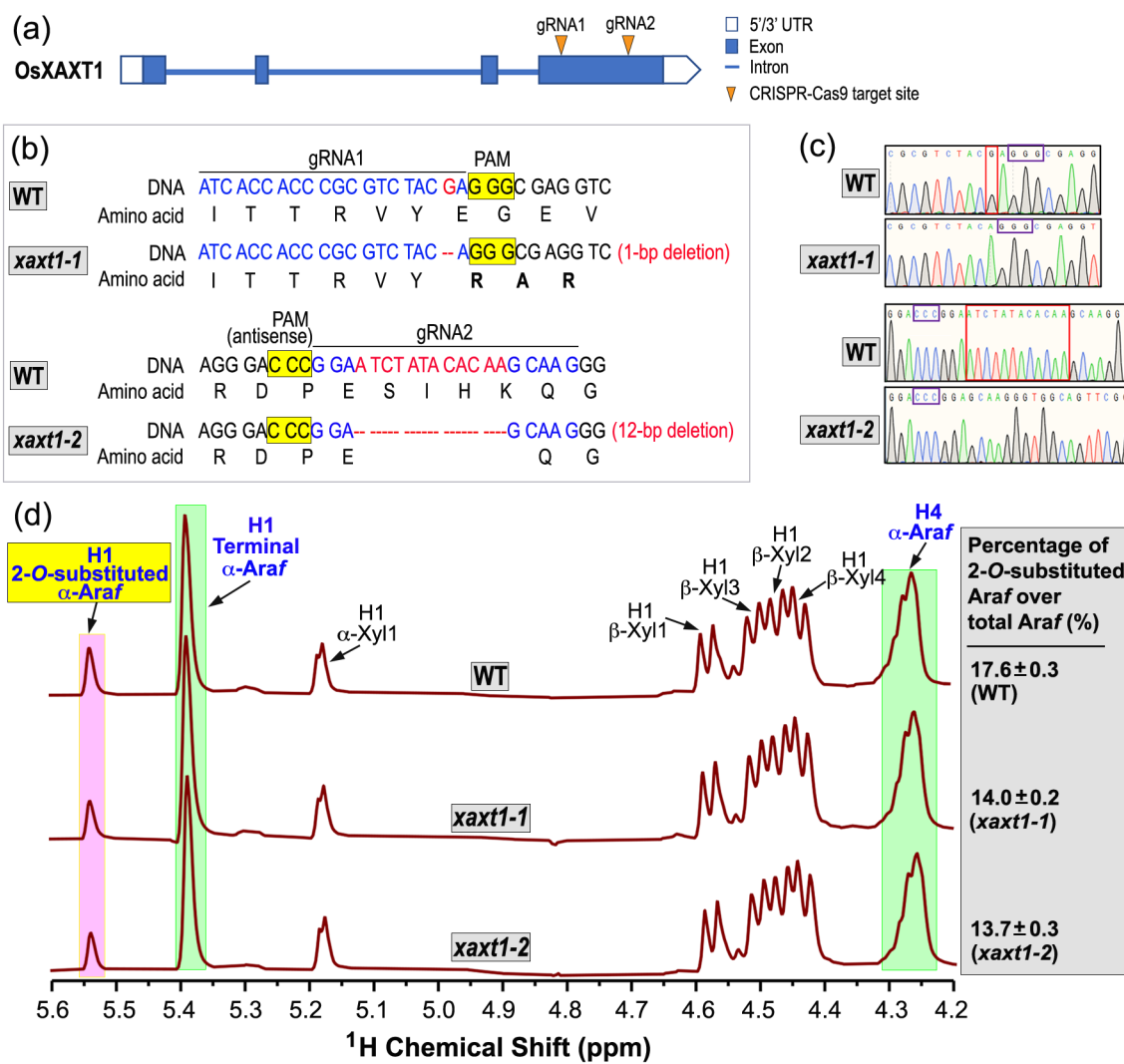
TPJ_15939_Fig.2-701-833-NMR copy.tif



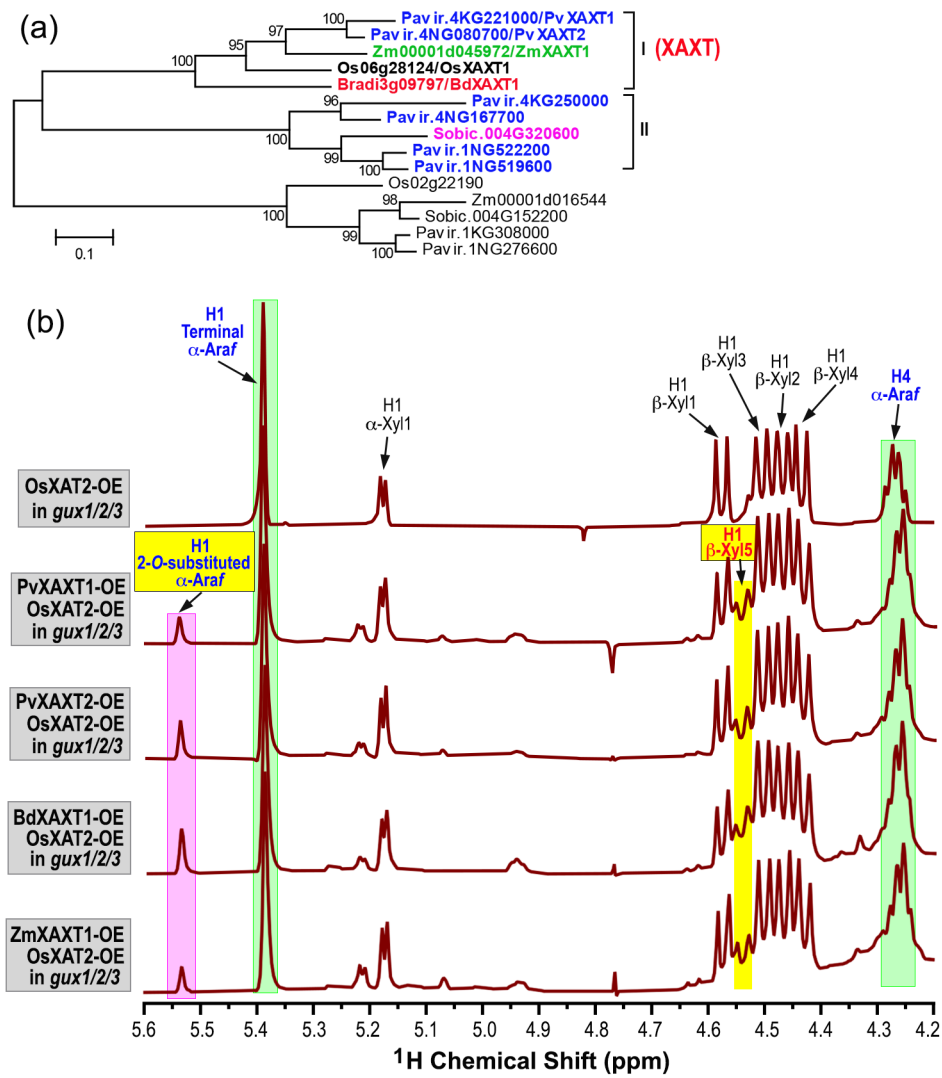
TPJ_15939_Fig.3-2D-NMR copy.tif



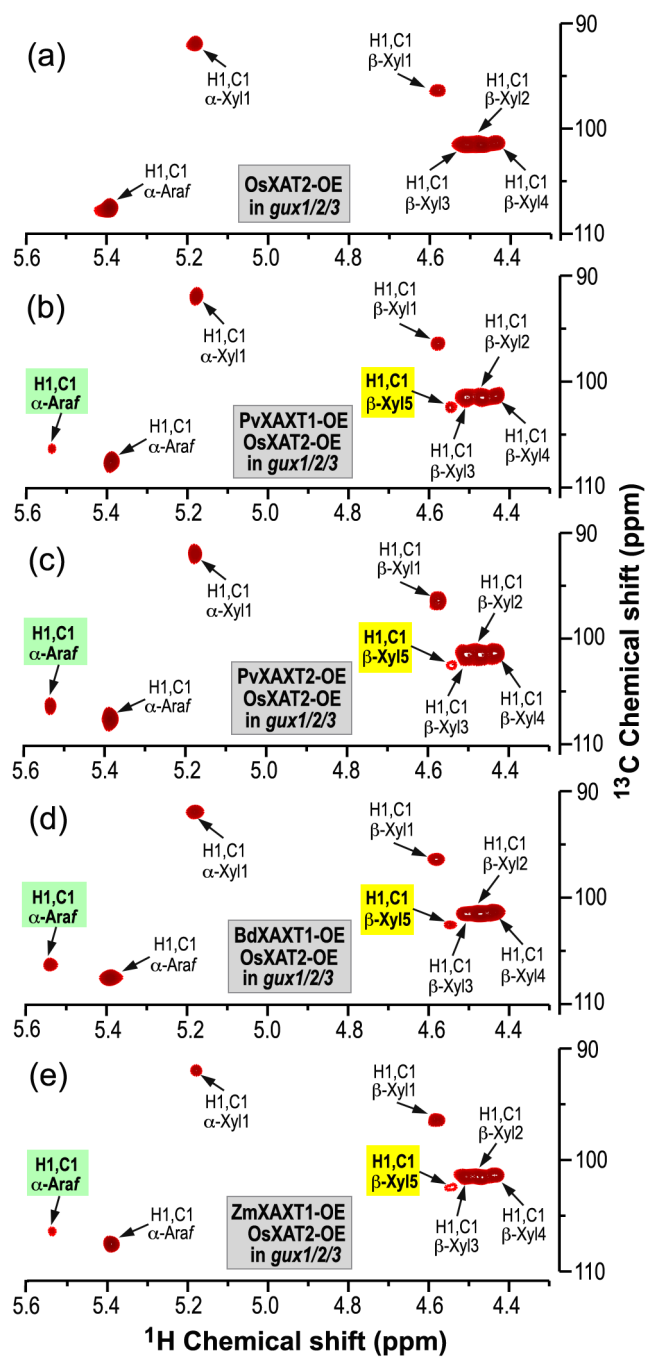
TPJ_15939_Fig.4-GFP-Activity copy.tif



TPJ_15939_Fig.5-Crispr-cas9 copy.tif



TPJ_15939_Fig.6-grass G1-NMR copy.tif



TPJ_15939_Fig.7-NMR-2D copy.tif